A Molecular Dynamics Study of Liquid Cesium Along Vapour Pressure Curve

S. Ranganathan[a]; K. Tankeshwar[b]; K. N. Pathak[a]

[a] Department of Mathematics and Computer Science, Royal Military College of Canada, Kingston, Ontario, Canada [b] Centre of Advanced Study in Physics, Department of Physics, Punjab University, Chandigarh, India

PLEASE SCROLL DOWN FOR ARTICLE

A MOLECULAR DYNAMICS STUDY OF LIQUID CESIUM ALONG VAPOUR PRESSURE CURVE

S. RANGANATHAN [a], K. TANKESHWAR [b] and K. N. PATHAK [b],*

[a] Department of Mathematics and Computer Science, Royal Military College of Canada, Kingston, Ontario K7K 5LO, Canada;
[b] Centre of Advanced Study in Physics, Department of Physics, Punjab University, Chandigarh 160014, India

Molecular dynamic simulation of liquid cesium along its vapour pressure curve has been done using Ichimaru-Utsumi potential. This potential have been compared with PST and DRT potential near the triple point. We have studied static pair correlation function, time evolution of velocity auto-correlation function, and self diffusion coefficients for four thermodynamic states. It is found that the position of first peak in pair correlation function almost remains same whereas its peak height decreases as temperature is increased. The calculated values of the self-diffusion coefficient have been compared with experimental result wherever available. Using the MD values of reduced diffusion coefficients for expanded Rb and present results for expanded Cs, it is predicted that both data can be represented by a single straight line as a function of reduced density and temperature.

Keywords: Self-diffusion; expanded cesium; molecular dynamics simulations

1. INTRODUCTION

There has been extensive computer simulation studies of structure and dynamics of liquid Lennard Jonesium over a wide range of densities and temperatures. In case of liquid metals such studies were limited to mostly at triple points. There were two reasons for this. Firstly, it was due to the scarcity of experimental data on static and dynamic

---

*Corresponding author.

correlation functions for different thermodynamics states. Secondly, the non-availability of reliable interatomic potential for liquid metals as a function of density which is the only required input in computer simulation studies. However, at present the situation is much better for liquid alkali metals. This is due to the recent studies [1 – 4] for static and dynamical properties by performing neutron scattering experiments on expanded Rb and Cs. Secondly, due to the simplicity of their electronic strucutre in solid phase which is nearly free electron like, one can obtain an effective ion-ion interaction potential within the framework of pseudo potential formalism [5, 6]. For alkali metals, effective ion-ion potential has been found to provide reasonable descriptions of their properties in the solid state as well as to limited extent in the liquid state.

In an earlier paper [7] we have studied the potential effects on some liquid state properties of cesium and sodium at their triple point using two different potential labeled as DRT (Dagens, Rasolt and Taylor [8]) and PST (Price, Singwi and Tosi [9]) potentials. In this paper a somewhat different version of PST potential is used. The present version of potential also uses Ashcroft [10] one parameter pseudo potential and the dielectric screening function of Ichimaru-Utsumi [11] with some what different value of pseudo potential parameter r_c than used by Price, Singwi and Tosi. The so called Ichimaru and Utsumi potential has been also used to study [12] the both the solid state and liquid state properties of cesium with acceptable results. This potential has also been used to study the structure of cesium along vapour pressure curve and simulation results have been found to be in agreement with diffraction experiments for static structure factors for liquid alkali metals by varying the values of parameter, r_c.

The motivation of the present study is to predict some dynamical properties of cesium along vapour pressure curve by using IU potential with value of r_c which has provided good results for solid/liquid state properties at the triple point. With this potential we calculate the static pair correlation function, velocity auto-correlation function, mean square displacement for cesium along vapour pressure curve. Results at triple point are compared with available experimental data and good agreement has been achieved. The second objective of the present work is to establish the scaling behavior of reduced diffusion coefficient as a function of reduced density and temperature

for expanded alkali metals, similar to known behavior [13] for liquid
metals at triple point. In order to do this we will use the present results
for expanded Cs and earlier MD results [14, 15] for expanded Rb, both
of which have been obtained by employing the same form of the
interaction potential.

In section 2 we describe the IU potential used in the present work
and compare with PST potential. For completeness we also compare
these potential with Dagens, Rasolt and Taylor (DRT) potential. The
property of this potential is that it does not contain any adjustable
parameter and also provided acceptable results for solid/liquid state
properties at triple point. We present some details of our molecular
dynamics simulation in section 3. Results and discussion are given in
section 4. The paper is concluded in section 5 along with the summary
of the work.

2. INTERATOMIC POTENTIAL

Three interatomic potential mostly used for liquid alkali metals at
their triple point are presented in Figure 1 for completeness and future
reference. The continuous, dashed-dot and dashed lines respectively
denote IU, PST and DRT potential. The well depth ε and the position
of first zero of the potential, σ is different for each potential. These and
some other relevant data are given in Table I. It may also be noted the
value of pseudo potential parameter r_c (in units of Bohr radius) in 2.62
and 2.72 for PST and IU potential. With different electron gas
screening function for PST and IU potential, the above mentioned
values of r_c have produced the best fit for solid state phonons for
cesium. In Figure 2(a) IU potential is plotted for $r_c = 2.62$ and 2.72 for
comparison. The value of r_c have changed both ε and σ but the shape
of potential is practically the same. In Figure 2(b) plot of IU with
above values of r_c in dimension less unit shows only minor difference.
In Figure 3 we plot IU potential for cesium along vapour pressure
curve for $r_c = 2.72$. The continuous, dashed, dots and dashed dot lines
denote the potentials for four thermodynamic states corresponding to
(n^*, T^*) for (0.767, 0.58), (0.636, 0.130), (0.451, 1.93) and (0.322, 1.88)
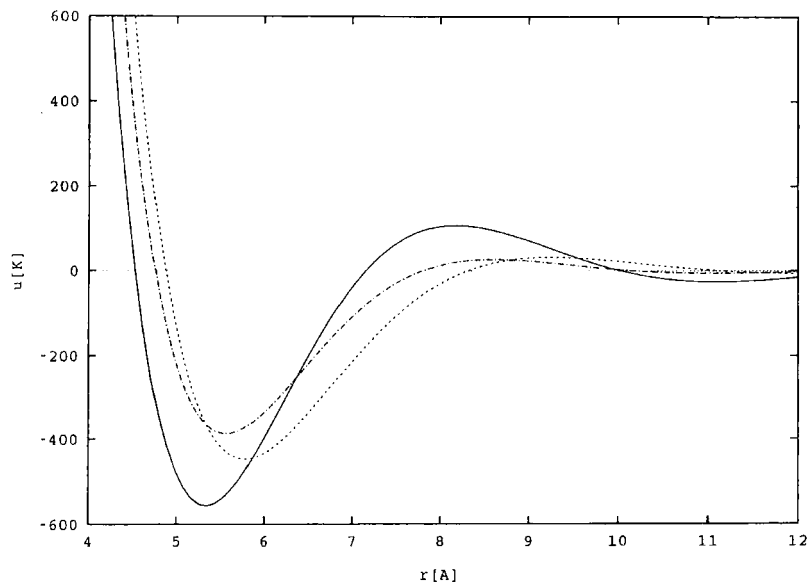which are labeled as states I, II, III and IV. $n^* (= n\sigma^3)$ and $T^* (= k_B T/\varepsilon)$

FIGURE 1   The interatomic potential in Kelvin (U/k_B) plotted as a function of r (in A) for Cs near its triple point. The continuous, dashed-dot and dashed lines, respectively, denotes IU, PST and DRT potentials.

TABLE I   Parameters of the IU potential. Values in the curved and square brackets correspond to DRT and PST potentials

State	$T(K)$	$n(A^{-3})$	$\sigma(A)$	$\varepsilon(K)$	$\tau(ps)$
I	323	0.00824	4.5315	557.166	2.436
			(4.878)	(447.1)	(2.927)
			[4.761]	[386.5]	[3.027]
II	773	0.00707	4.4808	594.789	2.331
III	1373	0.00545	4.3576	709.906	2.075
IV	1673	0.00432	4.2074	886.007	1.790

are reduced density and temperature. As the density increases along vapour pressure curve, the well depth and position of first zero of the potential increases and decreases separately. These potentials are used in computer studies presented in this work along the vapour pressure curve of Cs.
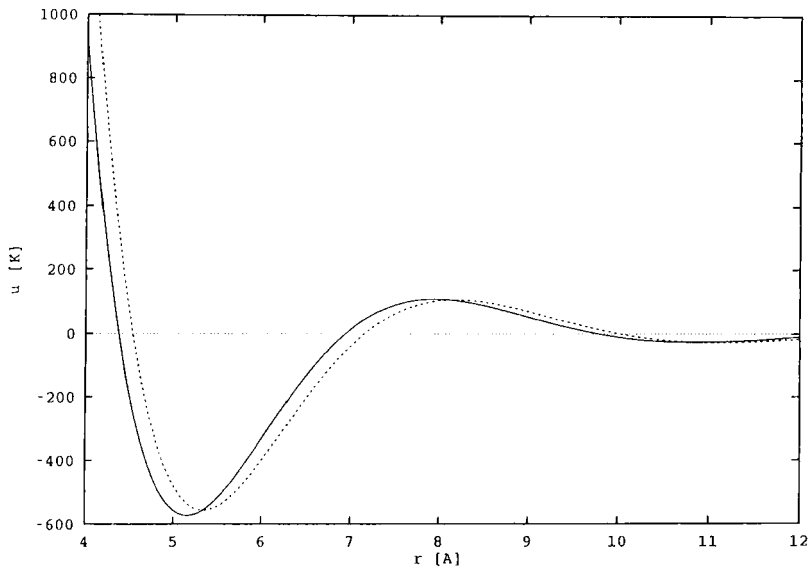
FIGURE 2a   The IU potential in Kelvin (U/k_B) plotted as a function of r (in A) for Cs near its triple point. The continuous and dashed lines, respectively, are for $r_c = 2.72$ and 2.62.

FIGURE 2b   The IU potential in reduced units ($U^* = U/\varepsilon$) plotted as a function of r (in A) for Cs near its triple point. The continuous and dashed lines, respectively, are for $r_c = 2.72$ and 2.62.
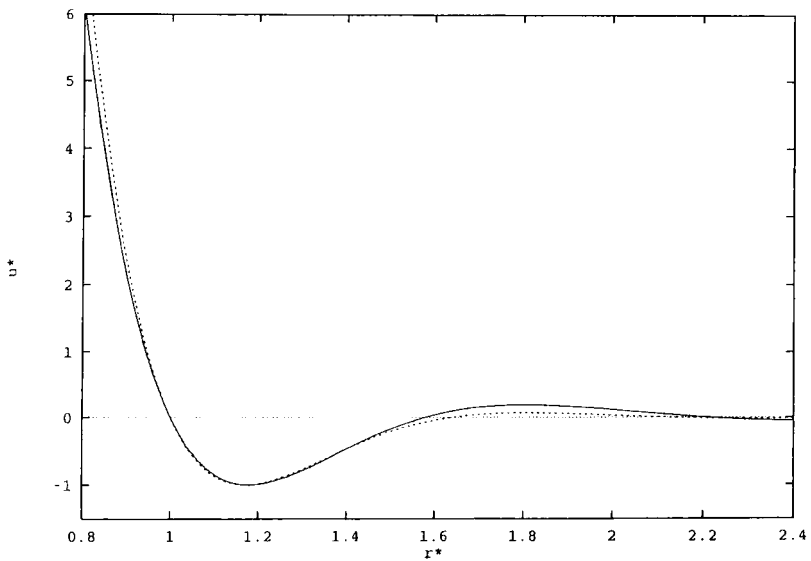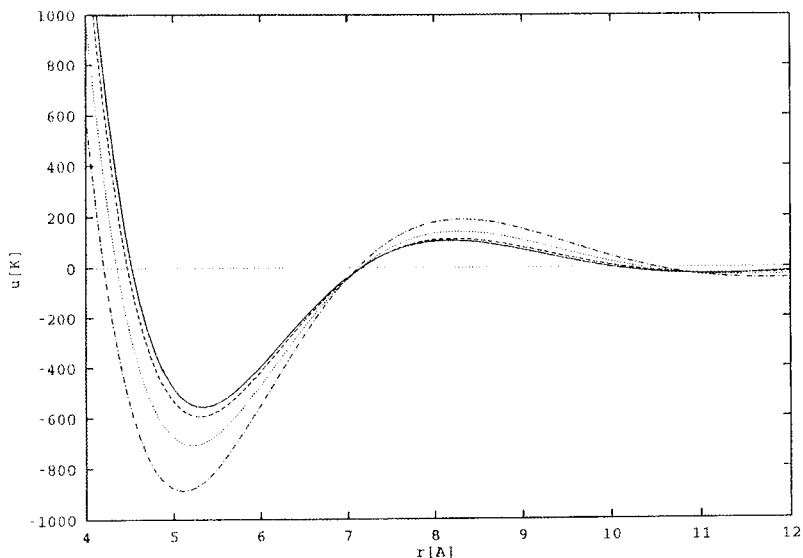
FIGURE 3   The IU potential in Kelvin (U/k_B) plotted as a function of r (in A) for Cs along vapour pressure curve for $r_c = 2.72$. The continuous, dashed, dots and dashed-dots lines denote the potential for four thermodynamic states corresponding to states I, II, III and IV, respectively.

3. MOLECULAR DYNAMICS CALCULATIONS

The molecular dynamics simulation have been carried out for system of 250 particles of cesium atoms cach of mass $m = 222.11 \times 10^{-24}$ gm along the vapour pressure curve. Relevant density and temperature are given in Table I for four thermodynamics states studied. The particles are confined to a cubic box of length $L = (N/n^*)^{1/3}\sigma$. The length of boxes are $6.88\,\sigma$, 7.32σ, $8.21\,\sigma$ and 9.19σ for $n^* = 0.767$, 0.636, 0.451 and 0.322, respectively. The time scale $\tau = \sqrt{m\sigma^2/\varepsilon}$ is used as unit of time, t. Using periodic boundary conditions, Newton's equation of motion have been solved employing the Verlet algorithm. The time steps for integration used is $\Delta t^* = 0.0046$ which corresponds a time increment of 2.435×10^{-14} s at 323 K. The temperature is controlled by scaling the velocities every 50 time steps and equilibrium was considered to be achieved if the temperature fluctuation was within 2 K. The equilibrium temperatures thus obtained are 323, 773, 1373 and 1673 K.

Once the equilibrium has been achieved, a MD run has been carried out for 8000 time steps. The position and velocity vectors $r(t)$ and $v(t)$ are stored for calculation of correlation function.

4. RESULTS AND DISCUSSION

4.1. Static Correlation

The results obtained for pair correlation function near the triple point (state I) are shown in Figure 4. The solid and dashed lines represent results at $r_c = 2.72$ and 2.62, respectively. The experimental results [16] are shown there as diamonds. MD results for $r_c = 2.72$ are more closer to the experimental results as can be seen from the position of first maxima in $g(r)$. Therefore, for further calculations we use $r_c = 2.72$. The results obtained for $g(r)$ and $S(q)$ at states II, III and IV are given in Figures 5 and 6, respectively. It can be seen from Figures 5 and 6 that positions of first maxima in $S(q)$ and $g(r)$ effectively remain at same point for all the thermodynamic states. However, the peak height
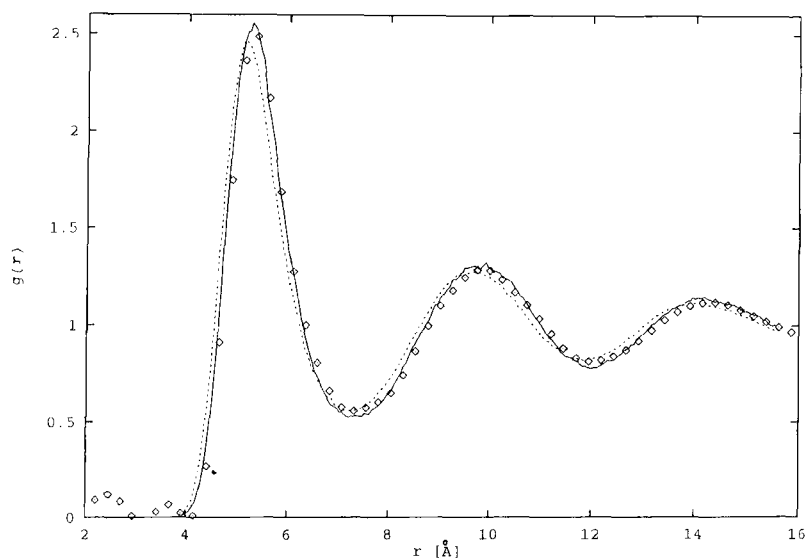

FIGURE 4   Static pair correlation function $g(r)$ vs r in Angstrom at state I, Solid and dashed lines corresponds to $r_c = 2.72$ and $r_c = 2.62$, respectively. The symbols represent the experimental data.
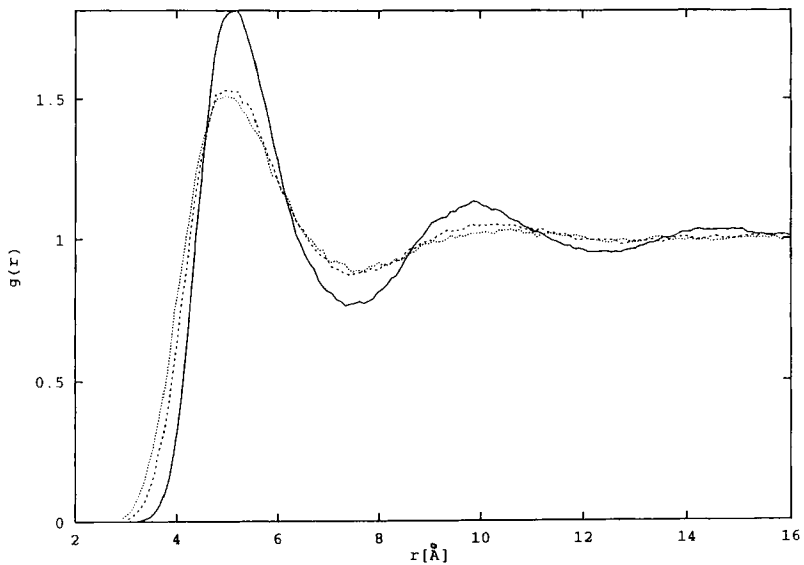
FIGURE 5 Variation of $g(r)$ vs r. Solid, dashed and dotted lines are for thermo-dynamic states II, III and IV, respectively.
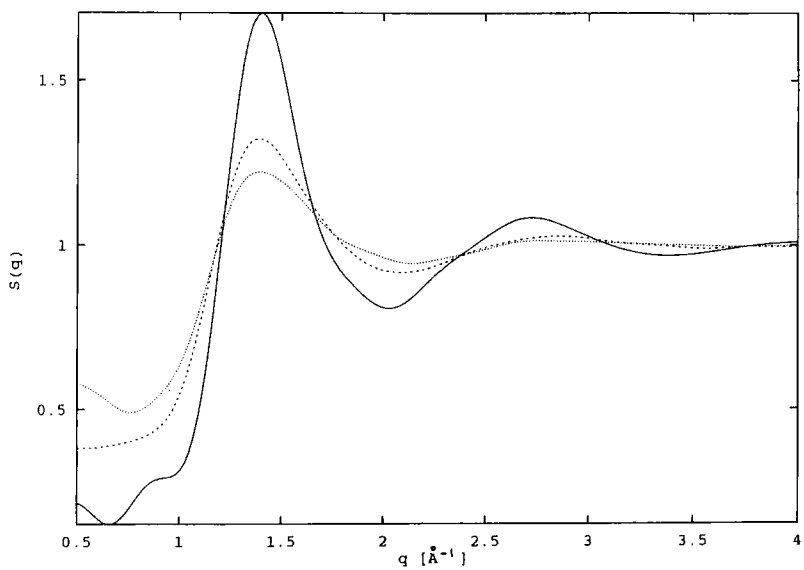

FIGURE 6 Variation of $S(q)$ vs q. Solid, dashed and dotted lines are for thermo-dynamic states II, III and IV, respectively.

decreases as one increases the temperature. This implies that during the expansion the nearest neighbor distance remains the same whereas the numbers of nearest neighbors decreases as one approach the critical point. This observation is consistent with experiments [3, 4] and MD simulation [14] on Rb.

4.2. Self-Diffusion Coefficients

The self-diffusion coefficient of tagged particle can be obtained from the mean square displacement

$$D = \lim_{t \to \infty} \langle |r_i(t) - r_i(0)|^2 \rangle / 6t \tag{1}$$

or from the velocity auto-correlation function

$$D = \frac{1}{N} \int_0^\infty \langle v_i(t) v_i(0) \rangle dt. \tag{2}$$

The MD results obtained for the normalized velocity auto-correlation function, $C(t)$ for four thermodynamic states are plotted against t^* in Figure 7. From the figure it can be seen that for two thermodynamics states $C(t)$ show negative minima whereas for two higher temperatures, $C(t)$ decay monotonically. This could be understood from the so-called cage effects. The cage is formed by neighboring particles of the tagged particle. The tagged particle gets reflected within the cage and forms a negative region in the time development of the velocity auto-correlation function. At higher temperature cages become larger and finally disappear then the $C(t)$ decays without oscillations.

In Figure 8 we plot mean square displacement $\langle r^2(t) \rangle$ versus t^*. It can be seen from the figure that initially the mean square displacement increases parabolically corresponding to free particle dynamics. At larger time $\langle r^2(t) \rangle$ becomes essentially linear and slope of which determines the diffusion coefficient. The values of the self-diffusion coefficients from Eq. (1) are given in Table II. It was also noted that Eqs. (1) and (2) essentially provide the same value of self-diffusion coefficients. The experimental value [17] available at triple point is given in bracket in Table II. It is seen that agreement is quite close.
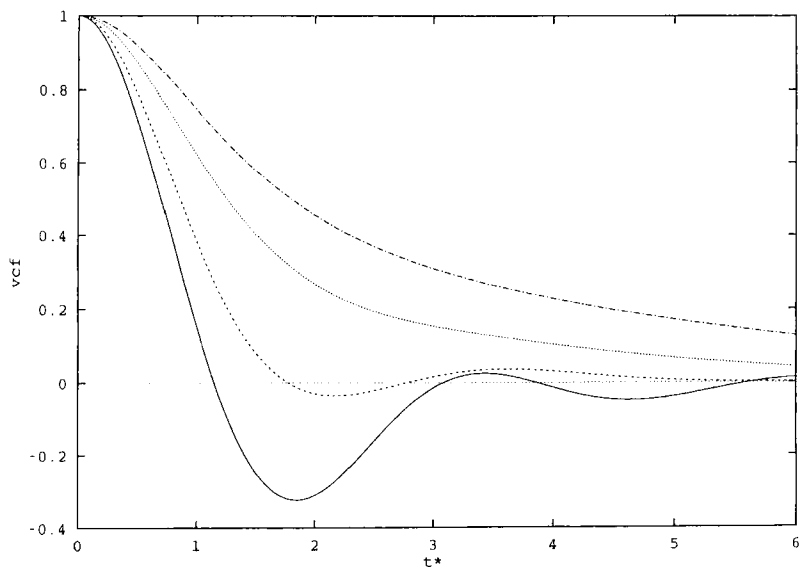
FIGURE 7   Variation of normalized VCF, C(*t*) vs *t**. Solid, dashed, dotted and dashed-dots lines are for thermodynamic states I, II, III and IV, respectively.
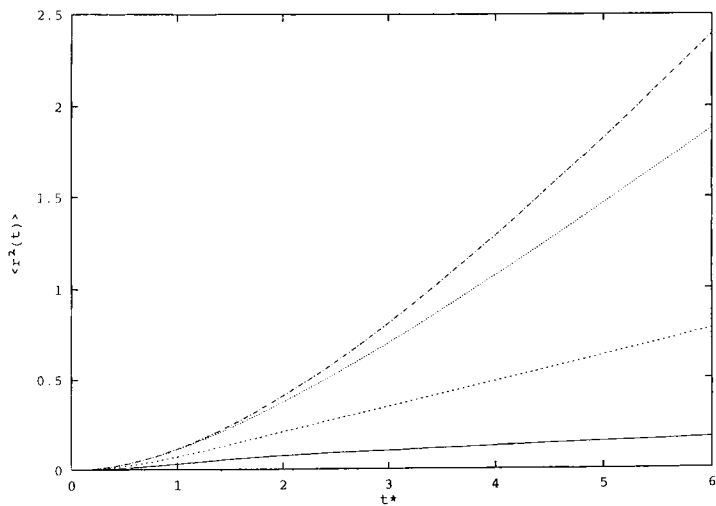

FIGURE 8   Variation of mean square displacement $\langle r^2(t) \rangle$ vs *t**. Solid, dashed, dotted and dashed-dots lines are for thermodynamic states I, II, III and IV, respectively.

In order to establish the relation between $D^* = D\tau/\sigma^2$ and n^* and T^*, in Figure 9 we plot D^* versus $\sqrt{T^*}/n^*$ for expanded Rb (circles) and Cs (squares). The MD values for the Rb are taken from the work of Kahl [14] along with corresponding values of ε and σ given by Sharma and Tankeshwar [18]. From the figure it can be seen that D^* is linear in

TABLE II   Values of the self-diffusion coefficients $D(10^{-4}\text{cm}^2/\text{sec})$. The value in the bracket represents experimental result

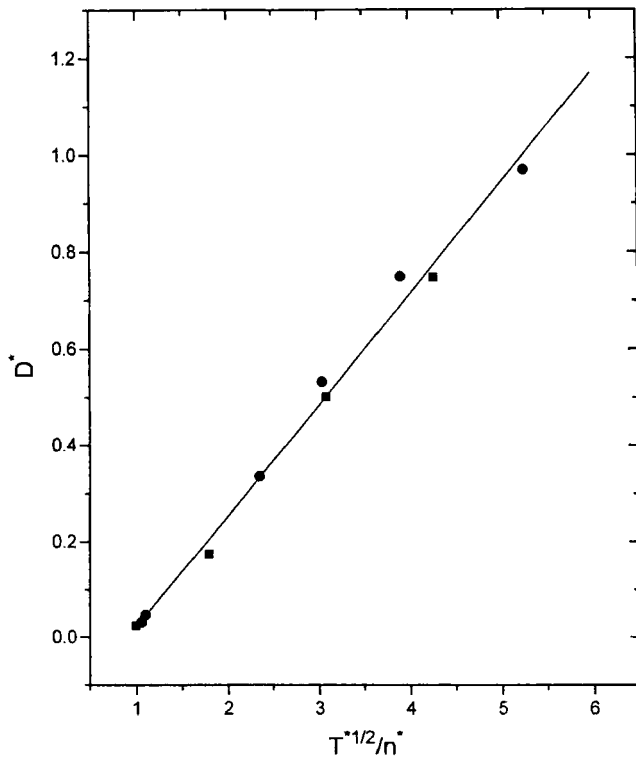| state	I	II	III	IV
D	0.21 (0.216)	1.5	4.6	7.4

FIGURE 9   Reduced self-diffusion coefficient versus $\sqrt{T^*}/n^*$. Filled circles and squares represent MD data for Rb and Cs. Straight line corresponds to Eq. (3).

$\sqrt{T^*}/n^*$. This solid line in Figure 9 can be well represented by

$$D^* = 0.229652 \frac{\sqrt{T^*}}{n^*} - 0.20593. \tag{3}$$

The representation of data by a single straight line for diffusion coefficients for different thermodynamic states for liquid Rb and Cs implies that there exist a kind of scaling of diffusion coefficients as has already been noted in alkali metals [13] near the triple point.

5. SUMMARY AND CONCLUSION

In this paper we have done computer simulation to study the static pair correlation function, velocity auto correlation and self-diffusion of expanded cesium for four thermodynamics states along the liquid-vapour co-existence curve by using Ichimaru-Utsumi potential. We have also compared the IU potential with the PST and DRT potentials. Results obtained for static correlation near the triple point have been compared with the available experimental results and a good agreement have been found. It is found that the first peak position in $g(r)$ and $S(q)$ remains almost same whereas the peak height decreases as temperature increases. The results obtained for the self-diffusion coefficients have been compared with experimental result available at triple point. The agreement is found to be very close. Using the earlier MD values of reduced diffusion coefficients for expanded Rb and present results for expanded Cs, it is predicted that both data can be represented by a single straight line as a function of reduced density and temperature.

References

[1] Pilgrim, C., Winter, R., Hensel, F., Morkel, C. and Glaser, W. (1992). *Recent Developments in Physics of Fluids*, Eds. W. S. Howells and A. K. Soper (Bristol: Hilger), p F181.
[2] Winter, R., Pilgrim, C., Hensel, F., Morkel, C. and Glaser, W. (1993). *J. Non. Cryst. Solids*, **158–58**, 9.

[3] Franz, G., Freyland, W., Glaser, W., Hensel, F. and Schneider, E. (1980). *J. Physique Coll*, **41**, C8.
[4] Winter, R., Bodensteiner, T., Glaser, W. and Hensel, F. (1987). *Ber. Bunsenges, Phys. Chem.*, **91**, 1323.
[5] Hansen, J. P. and McDonald, I. R. (1989). *Theory of Simple Liquids*, (Academic, New York).
[6] March, N. H. (1990). *Liquid Metals: Concepts and Theory*, Cambridge University Press, Cambridge.
[7] Ranganathan, S., Pathak, K. N. and Varshni, Y. P. (1994). *Phys. Rev.*, **E49**, 2835.
[8] Dagen, L., Rasolt, M. and Taylor, R. (1975). *Phys. Rev.*, **B11**, 2726.
[9] Price, D. L., Singwi, K. S. and Tosi, M. P. (1970). *Phys. Rev.*, **B2**, 2983.
[10] Ashcroft, N. W. (1966). *Phys. Lett.*, **23**, 48.
[11] Ichimaru, S. and Utsumi, K. (1981). *Phys. Rev.*, **B24**, 7385.
[12] Kambayashi, S. and Kahl, G. (1992). *Phys. Rev.*, **A46**, 3255
[13] Ranganathan, S. and Pathak, K. N. (1994). *J. Phys.; Codens. Matter*, **6**, 1309.
[14] Kahl, G. and Kambayashi, S. (1994). *J. Phys.: Condens. Matter*, **6**, 10897.
[15] Kahl, G. (1994). *J. Phys.: Condens. Matter*, **6**, 10923.
[16] Waseda, Y. *The structure of Non-Crystalline Materials: Liquids and Amorphous Solids*, (McGraw-Hill, New York, 1980).
[17] Gerl, M. and Barson, A. (1985). *Handbook of Thermodynamics and Transport Properties of Alkali Metals* Ed. R. W. Ohse (Oxford: Blackwell Scientific.) 845.
[18] Sharma, Saroj K. and Tankeshwar, K. (1996). *J. Phys.: Condens. Matter*, **8**, 10839.